Seismic Deconvolution Using Sparse Spike Inversion vs. Basis Pursuit Inversion

Deborah Pereg and Israel Cohen, Technion – Israel Institute of Technology, and Anthony A. Vassiliou, GeoEnergy, Inc.*

SUMMARY

In this paper, we compare two methods for seismic inversion - Sparse Spike Inversion (SSI) and Basis Pursuit Inversion (BPI). Both methods utilize sparse inversion techniques. We employ a Least-Angle Regression (LARS) Least Absolute Shrinkage and Selection Operator (LASSO) solver for their implementation. Experimental results confirm that L1 penalization in the LASSO optimization improves the performance in terms of recovering reflection coefficients.

INTRODUCTION

Deconvolution is a signal processing operation that, ideally, unravels the effect of a convolution performed by a linear time invariant system operating on an input signal. In seismic deconvolution, a short seismic pulse is transmitted from the earth surface. The reflected pulses from the ground are received by a sensor array. Our goal is to reveal the ground layer's structure hidden in each of the received seismic traces.

A short seismic pulse (wavelet) is assumed to be known. (Practically, it is pre-estimated). Even if the wavelet is known, the inversion process is often unstable. The seismic wavelet is bandlimited, and the seismic trace might be noisy. Therefore, there are many possible reflectivity series that could fit the same measured seismic traces. Our objective is to find the best estimate of the reflectivity. We assume the reflectivity is sparse. Hence, its extraction could be done by sparse inversion techniques.

Sparse seismic inversion methods can produce stable reflectivity solutions that contain frequencies that are not contained in the original signal, without necessarily magnifying the noise in these signals, see e.g., Riel and Berkhout (1985). However, these methods usually rely on a-priori knowledge that is employed for increasing the resolution beyond the resolution offered by wavelet inverse filtering. Typically, a starting model is built by spatially interpolating well logs along selected horizons. Unfortunately, lateral changes in the waveform interference pattern, or in the velocities or impedances, can result in incorrect starting model and an erroneous inversion.

Matching pursuit decomposition (MPD) (see Nguyen and Castagna (2010)) decompose the seismic trace into a superposition of reflectivity patterns. The MPD has some limitations especially when the dictionary elements are not orthogonal.

Basis pursuit decomposition (BPD) (Chen *et al*. (2001)) has many advantages over MPD. BPD was originally developed as a compressive sensing technique, which utilizes an L1 norm optimization. It finds a single global solution, whereas MPD is a path dependent process. Moreover, it is computationally more efficient, and as BPD introduces a sparsity norm and a regularization parameter into the objective functions, it can exhibit good lateral stability even when dictionary elements are not orthogonal.

In this study, we investigate two methods Sparse Seismic Inversion and Basis Pursuit Inversion, see Zhang and Castagna (2011), Taylor *et al* (1979). In the following, we briefly present the models and the solution approaches, and refer the reader to Zhang and Castagna (2011), Taylor *et al* (1979) for further details.

The remainder of the paper is organized as follows. First, we review the basic theory of the two methods. Then, we describe our experiments with synthetic and real data. Lastly, we conclude and discuss further research.

METHODOLOGY

We can model $s(t)$, the received seismic signal (the observation) as

$$s(t) = w(t) * r(t) + n(t) \tag{1}$$

where $w(t)$ is the seismic wavelet, $r(t)$ is the reflectivity series, and $n(t)$ is the noise. The symbol $*$ denotes one-dimensional linear convolution operation. This model assumes that the earth structure can be represented by planar horizontal layers of constant impedance, so that reflections are generated at the boundaries between adjacent layers. Each 1D seismic trace is a convolution of the seismic wavelet and the reflectivity pattern.

The objective is to find an estimate of the reflectivity $r(t)$. The reflectivity is assumed to be sparse as only boundaries between adjacent layers may cause a reflection of the seismic wave.

As (1) implies, the seismic trace consists of a linear combination of w(t) and its time shifts, according to the non-zero reflectors in $r(t)$. After time discretization, and an addition of random noise, (1) can be written in matrix-vector form as follows

$$s_{N\times1} = W_{N\times M} r_{M\times1} + n_{N\times1} \tag{2}$$

where $W_{N\times M} \in \mathbb{R}^{N\times M}$, also known as the dictionary.

In the Sparse Spike Inversion (SSI) method $W_{N\times M}$ is the convolution matrix formed by the seismic discrete wavelet $w(t)$. The inversion problem of finding $r_{M\times1}$ from the noisy measurement $s_{N\times1}$ is formulated as

$$\min \|r_{M\times1}\|_0 \text{ subject to } \|s_{N\times1} - W_{N\times M} r_{M\times1}\|_2^2 < \varepsilon. \tag{3}$$

After relaxing L0 to L1-norm we obtain the constraint:

$$\min_{r_{M\times1}} \frac{1}{2} \|s_{N\times1} - W_{N\times M} r_{M\times1}\|_2^2 + \lambda \|r_{M\times1}\|_1. \tag{4}$$

The problem formulated in the form of (4) is named Least Absolute Shrinkage and Selection Operator (LASSO) (see Tibshirani (2013)). The use of L1 penalty in similar problems promotes sparsity of the solution $r_{M\times1}$ (see Chen *et al.* (2001), Elad (2010)).

On the other hand, the Basis Pursuit Inversion (BPI) method, proposed by Zhang and Castagna (2011), utilizes dipole decomposition to represent the reflectivity series as a sum of even and odd impulse pairs multiplied by scalars. Each even and odd pair corresponds to the top and base reflector of a layer. Since the layer thickness is unknown, the dictionary comprises all possible thicknesses up to a maximum layer time-thickness.

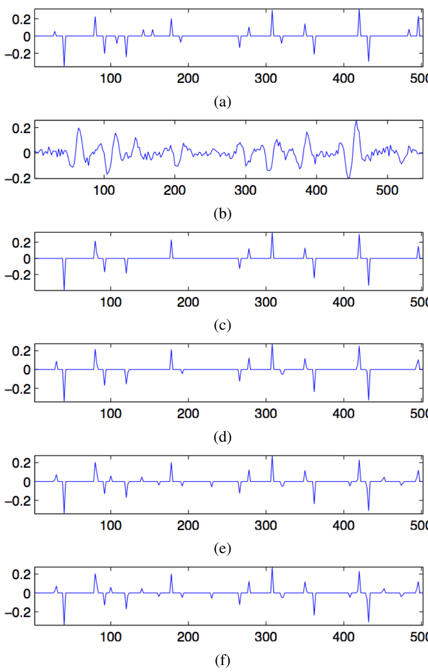

Figure 1: 1D synthetic tests of SSI. (a) True reflectivity. (b) Synthetic trace with 40 Hz Ricker wavelet and SNR= 10 dB. (c)-(f) SSI inversion results with varying λ_{SSI}. (c) $\lambda_{\text{SSI}} = 0.29$, (d) $\lambda_{\text{SSI}} = 0.11$, (e) $\lambda_{\text{SSI}} = 0.071$, (f) $\lambda_{\text{SSI}} = 0.025$.

Assuming the sample rate is Δt, each even wedge reflectivity can be written as

$$r_e(t,m,n,\Delta t) = \delta(t - m\Delta t) + (t - m\Delta t - n\Delta t) \tag{5}$$

and each odd wedge reflectivity can be written as

$$r_o(t,m,n,\Delta t) = \delta(t - m\Delta t) - \delta(t - m\Delta t - n\Delta t)\,. \tag{6}$$

Since any reflectivity can be written as

$$r(t) = \sum_{n=1}^{N}\sum_{m=1}^{M} a_{n,m} * r_e(t,m,n,\Delta t) + b_{n,m} * r_o(t,m,n,\Delta t) \tag{7}$$

the BPI dictionary consists of a convolution of the wavelet with the even wedge reflectivity and with the odd wedge reflectivity, and the objective is to calculate the coefficients $a_{n,m}$ and $b_{n,m}$.

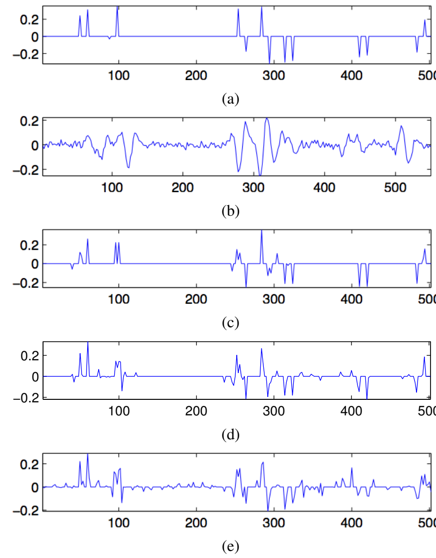

Figure 2: 1D synthetic tests of BPI. (a) True reflectivity. (b) Synthetic trace with 40 Hz Ricker wavelet and SNR= 10 dB. (c)-(f) BPI inversion results with varying λ_{BPI}. (c) $\lambda_{\text{BPI}} = 0.27$, (d) $\lambda_{\text{BPI}} = 0.087$, (e) $\lambda_{\text{BPI}} = 0.011$.

SYNTHETIC EXAMPLES

First, we evaluate the performances of the SSI and the BPI techniques with synthetic data. To test the methods, we used a 40 Hz Ricker wavelet and generated a reflectivity series with sample rate of 2 milliseconds.

To evaluate our result we used the normalized correlation coefficient:

$$\rho = \frac{\langle \hat{r}, r\rangle}{\|\hat{r}\|_2\,\|r\|_2} \tag{8}$$

where $\hat{r}(t)$ is an estimate of the reflectivity series.

A small modification to the Least-Angle Regression (LARS) algorithm can solve the LASSO problem, as described in Efrom *et al.* (2004). In our simulation, we use the SpaSM toolbox (Sjöstrand *et al.* (2012)) to implement the LASSO algorithm for both the BPI and SSI, as proposed by Rozenberg *et al* (2014).

A regularization parameter λ in (4) balances between the reflectivity sparsity and the noise. Increasing λ decreases the sparsity of the solution, whereas decreasing λ may cause noise amplification. Both SSI and BPI utilize λ as a trade-off factor that controls the inversion output. However, one cannot compare the values between the methods. Practically, the value of λ is data dependent and determined empirically.

Figures 1 and 2 show the SSI and BPI inversion results for a specific test. The non-zero reflection coefficients uniformly distributed between -0.2 and 0.2 (shown in Figure 1(b). Denote by D the time difference between consecutive non-zero reflectivity coefficients. Then D ranges between 10 milliseconds to 200 milliseconds, and the reflectivity sparsity p was set to 0.06. Figures 1(a) and 2(a) show the synthetic reflectivity.

Figures 1(b) and 2(b) show the synthetic traces, which are a result of convolution between the wavelet and the reflectivity. The signal-to-noise ratio (SNR) is quite high (SNR $= 10$ dB). Figures 1(c)-(f) and 2(c)-(f) show the results of each of the techniques with varying parameters.

The series of synthetic tests that we have done during our research indicate that the optimal correlation can be achieved using different λ values, depending on the channel characteristics: the number of reflectors, the layers' thicknesses, the channel sparsity, and the SNR.

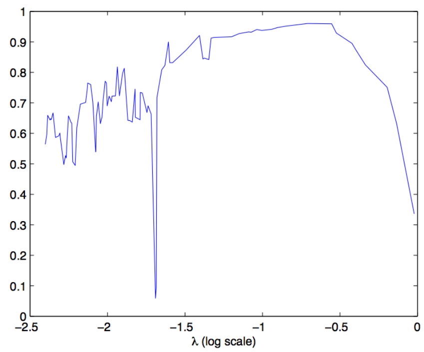

(a)

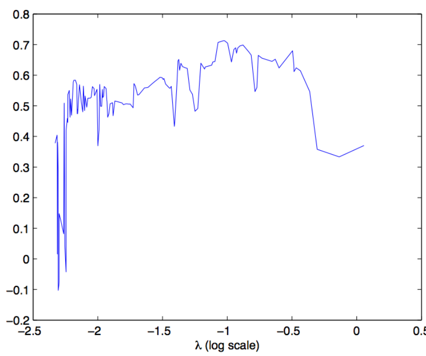

(b)

Figure 3: (a) λ-correlation curve for SSI based on the synthetic data in Figure 1. (b) λ-correlation curve for BPI based on the synthetic data in Figure 2.

Figure 3 presents the correlation coefficient for different λ values under the same conditions of SNR$= 10$ dB, and sampling rate of 2 milliseconds, for SSI and BPI methods.

REAL DATA RESULTS

The SSI inversion was tested on a 2D seismic data set shown in Figure 4. The estimated reflectivity, and seismic data reconstructed as a convolution between the estimated reflectivity and a given wavelet, are shown in Figure 5. The obtained correlation between the original and reconstructed seismic data is $_{s,\hat{s}} = 0.95$ for $\lambda_{\text{opt}} = 9.4 \times 10^{-3}$.

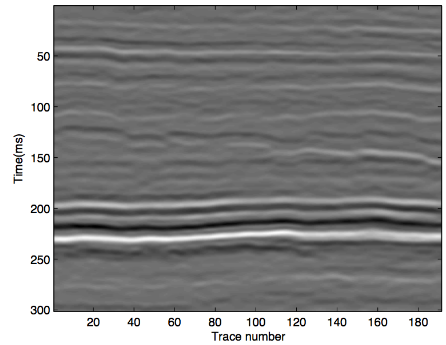

(a)

Figure 4: Seismic data.

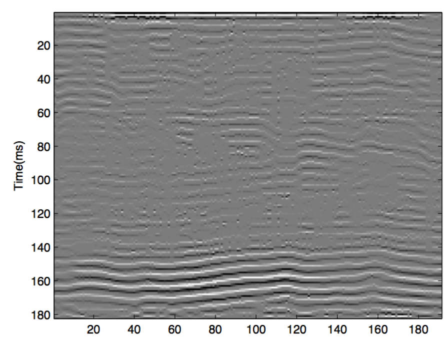

(a)

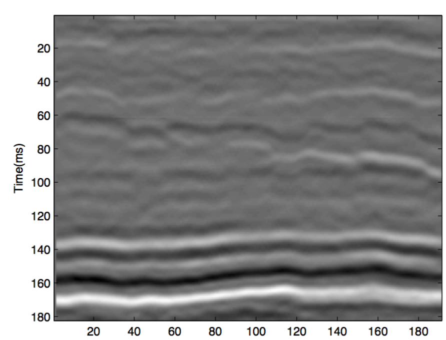

(b)

Figure 5: (a) Estimated reflectivity matrix; (b) Reconstructed seismic data.

CONCLUSION

The results presented in this paper reveal several interesting aspects of the sparse channel inversion methods. We used both synthetic and real data examples to evaluate the methods. Both methods yield reasonable estimates of the reflectivity under sufficiently high SNR. Our results indicate better performance of the SSI technique, although correct adjustments of the dictionary atoms selection can make the differences significantly smaller. We conclude that both methods could practically be used for seismic exploration and research purposes.

The choice of regularization parameter lambda is still an open problem. One needs to determine whether the resolution of the estimated reflectivity is real or a result of using a too small λ. In addition, in this study, we used a time-spatial-invariant known wavelet for simplicity. In practice, a time and spatial varying wavelet could improve the results, taking into account wave propagation effects, such as attenuation and dispersion.